MECSOL 2019 - Proceedings of the 7th International Symposium on Solid Mechanics,
V. Tita, A. Ferreira, M.L. Ribeiro, A. Vieira and A.T. Beck (Editors), ABCM, Sao Carlos, SP, Brazil, April 15th to 17th, 2019

On the importance of the filament winding pattern of composite cylinders in axial compression: damage and buckling analyses

Cristiano B. de Azevedo[1], José Humberto S. Almeida Jr.[2], Frederico Eggers[1], Heitor F. Flores[1], Sandro C. Amico[1]

[1]PPGE3M, Federal University of Rio Grande do Sul, Av. Bento Gonçalves 9500, 91501-970 Porto Alegre, RS, Brazil

[2]Mechanics and Composite Materials Department, Leibniz-Institut für Polymerforschung (IPF), Hohe Straße 6, 01069 Dresden, Germany

Abstract: Manufacturing characteristics of the filament winding process, such as formation of the winding pattern, are usually not taken into account in conventional numerical models. This paper deals with the evaluation of the influence of the filament winding pattern on buckling behavior in cylindrical shells subjected to axial compression loads. A nonlinear buckling model was developed, the damage initiation criteria were based on the Hashin theory, implemented in finite element software Abaqus. The modeling of the cylinders took into account the effect of the winding pattern. The numerical results were compared with experimental results previously tested, where it was verified that the nonlinear model provides a satisfactory prediction of the displacements over the loading history and the critical buckling load.

Keywords: buckling, post-buckling, filament winding pattern, composite cylinder

INTRODUCTION

Nowadays, the utilization and integration of fiber-reinforced composites into a variety of structural applications is continuously increasing. Filament wound (FW) composite cylinders made of carbon fiber-reinforced polymer (CFRP) have several advantages over cylinders made from conventional materials, such as high specific stiffness and strength, and high corrosion strength (Almeida Jr. et al., 2014). With the development of filament winding technology to produce FW cylinders, there has been a growing interest in application of FW cylindrical structures (Xia et al., 2001).

The process is based on winding continuous fiber rovings (also known as tows) onto a rotating mandrel. There are three possible winding trajectories: circumferential (or hoop), helical and polar (Almeida Jr. et al., 2016). In the helical winding, the rotational movement of the mandrel and the axial movement of the carriage produces a helical trajectory, where the full coverage occurs without the band having to be adjacent to the previously deposited band. Within the helical trajectory, two variants are possible: geodesic or non-geodesic. The geodesic path is the natural trajectory of the tow over a mandrel when there is no friction between the tow and the mandrel (Zu et al., 2013). A deviation from the geodesic path is when friction between the tow and the mandrel is considered, in which the higher the friction the higher the deviation on the tow placement. These characteristics result in a repetitive winding pattern, which results in a diamond architecture around the cylindrical surface. Each diamond consists of a unit cell (i.e., a periodic minimal unit), characterized by two distinct sections, each comprising half of the diamond and having continuous tows oriented at off-axis angles. Between these two sections, there is an undulation region where the fibers intersect themselves (Koussios, 2014), which is known as zig-zag area, as shown in Figure 1.

The architecture of these unit cells constitutes the filament winding pattern, which can be identified as a two-valued relationship "X/Y", which means that there exist X diamonds Y times around the circumference (Azevedo et. al., 2018). This means that within a particular winding angle it is possible to have several possible winding patterns. Consequently, it is still yet to be understood whether a FW cylindrical structure is winding pattern dependent. Figure 2 shows three examples of a cylindrical shell having a particular winding angle with different winding patterns.

Stress analysis of FW structures is usually performed based on the principles of Classical Laminate Theory (CLT). In these cases, a winding layer is considered as two homogenized angle-ply layers. The undulation region divides into circumferential and helical bands. The remaining triangular areas consist in stacked sets of unidirectional fibers, which are laminated alternatively in an $+\theta/-\theta$ orientation for one half and $-\theta/+\theta$ for the other half (Rousseau et al. 1999).

Only a few works have been found in the literature considering the winding pattern. Among them, Morozov (2006) analyzed numerically composite cylindrical shells under internal pressure considering the winding pattern. The results showed substantial differences in the stress values comparing the structures with and without modeling the pattern. In

addition, the stress distributions were not uniform along the length and circumference of the shell. For example, the maximum stress value acting along the fibers in the pattern 1/1 reached the stress levels between 10.0 and 40.9 MPa, whereas in the conventional model (without pattern) the maximum stress was 24.9 MPa. Mian et. al. (2011) modeled the winding pattern in pressure vessels subjected to internal pressure and compared with a conventional model. The stress levels in the model with pattern were higher than in the conventional model and the stress distributions were not uniform. For example, the stress value acting along the fibers in the conventional model were 21.5 MPa, and between 11.5 and 35.8 MPa in the winding pattern of 12/1.

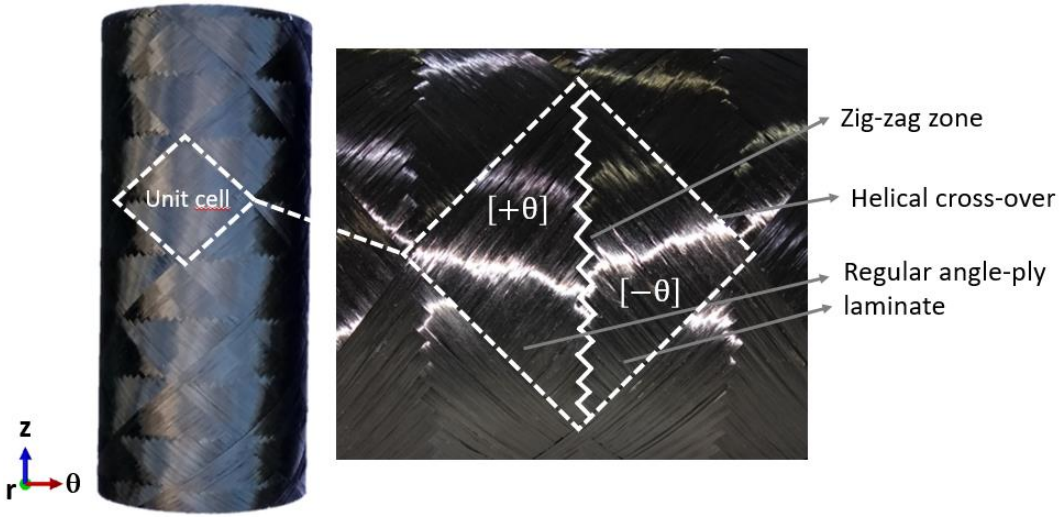

Figure 1 – Pattern architecture produced by helical winding.

In this context, the aim of this work is to evaluate the importance of the filament winding pattern on the mechanical response of composite cylinders under axial compression. A parametric analysis is carried out in order to understand the response of the cylinders when the modeling approach is non-linear buckling and progressive damage. The numerical predictions are compared with experimental results presented in (Azevedo et. al. 2019).

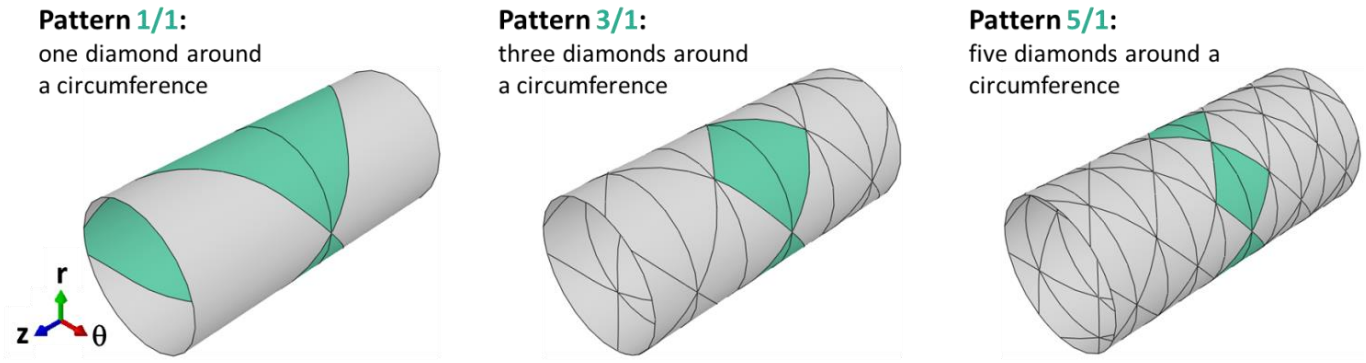

Figure 2 – Examples of different filament winding patterns.

FINITE ELEMENT MODELING

Winding pattern generation

The numerical models were developed in Abaqus™ 6.14 finite element (FE) package. The cylinders were modeled using a three-node reduced integration shell element (S4R) with equivalent single layer (ESL) formulation and hourglass control. This element is suitable for thin-walled shells and was chosen to reduce simulation time and avoid numerical issues. The material system used is a filament-wound unidirectional carbon/epoxy laminate composed of Toray T700-12K-50C carbon fiber and UF3369 epoxy resin. The engineering properties used here were obtained by Almeida et. al., 2016, (Table 1).

The modeling of the cylindrical shells incorporating the winding pattern was developed in Python language and linked with Abaqus. The model was elaborated according to the procedure described in detail in Azevedo et. al., 2018 and brief description is herein presented: Firstly, a cylinder with radius r and length l is drawn (Figure 3a). Next, reference datum

planes are created around the cylinder, containing lines that will form the mosaic pattern (Figure 3b). The positioning of these lines is defined from the considered winding pattern and trigonometric relations considering the winding angle. These lines are then projected onto the cylinder surface (Figure 3c). Similarly, vertical lines are created and projected to represent in a simplified way the circumferential undulation zone. These steps result in a complete modeling of the filament winding pattern (Figure 3d).

Table 1: Elastic and strength properties used in the FE models.

	Symbol	*Description*	*Value*
Elastic constants	E_1 (GPa)	Longitudinal elastic modulus	129.3
	$E_2 = E_3$ (GPa)	Transverse elastic modulus	9.11
	$\nu_{12} = \nu_{13}$	Poisson's ratio in plane 1-2 or 1-3	0.32
	ν_{23}	Poisson's ratio in plane 2-3	0.35
	$G_{12} = G_{13}$ (GPa)	In-plane shear modulus	5.44
	G_{23} (GPa)	Transverse shear modulus in plane 2-3	2.10
Strengths	X_t (MPa)	Longitudinal tensile strength	1409.9
	X_c (MPa)	Transversal tensile strength	− 740.0
	Y_t (MPa)	Longitudinal compressive strength	42.5
	Y_c (MPa)	Transversal compressive strength	− 140.3
	S_{12} (MPa)	In-plane shear strength	68.9

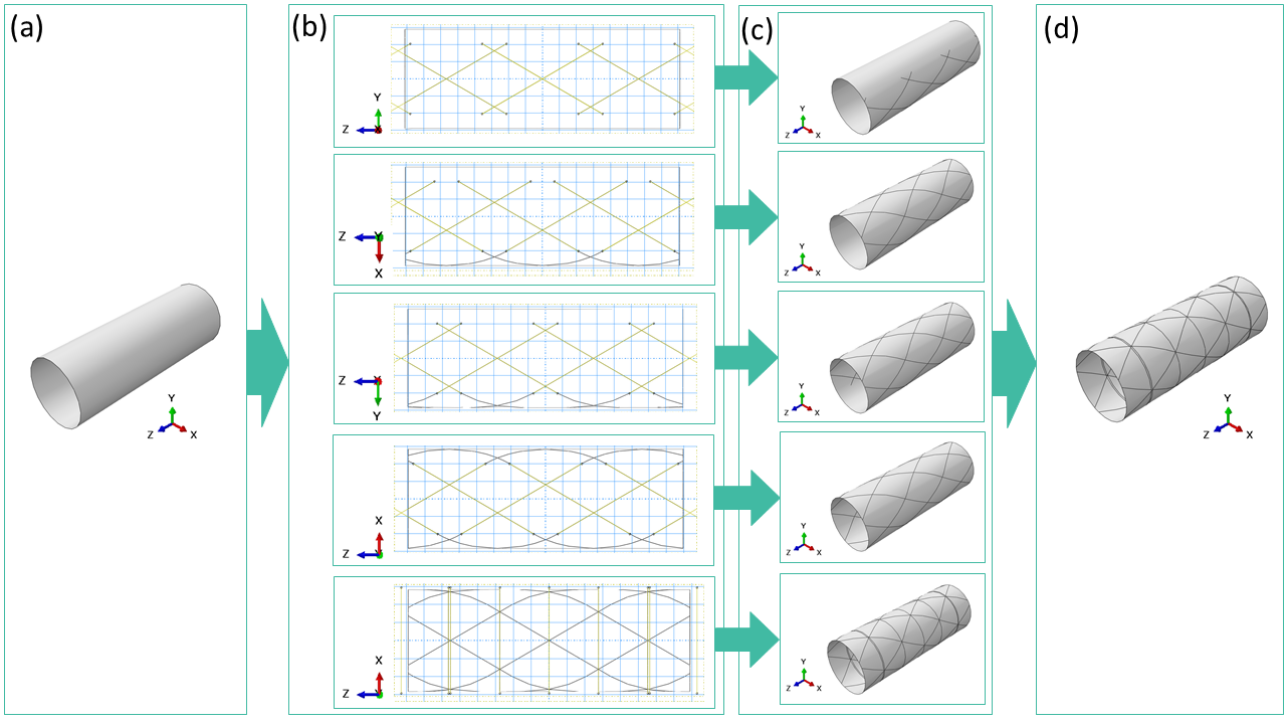

Figure 3 - Development stages of a particular winding pattern modeling: (a) cylinder modeling, (b) datum plane creation, (c) projection onto the cylinder surface and (d) complete cylinder modeling.

Non-linear buckling analysis

The buckling behavior of the cylinders was analyzed using the modified Riks method (Riks, 1979 and Crisfield, 1981).

The $[\pm 50]_{FW}$ cylindrical shells with r = 68 mm and l = 300 mm, winding pattern 1/1, 3/1 and 5/1 and thickness as experimentally determined in Azevedo et. al., 2019 (Table 2) were considered in the simulations (Figure 4).

The cylindrical shell was subjected to axial compression by contact with the compression plates, which were simulated as rigid bodies, and where the boundary conditions (BC) were imposed (Figure 5a). A node-to-surface contact algorithm was used to model plate-cylinder-plate interaction by using small sliding formulation with a friction coefficient of 0.15 between the plates and the cylinder. A reference point representing the upper compressive plate was created and its displacement was monitored and its reaction force has been collected throughout the simulation (Almeida Jr., et. al. 2018). The compressive plates were modeled using linear quadrilateral elements of R3D4 type (Figure 5b). A sensitivity analysis is previously performed using and the mesh is sufficiently refined in order to provide mesh-independent predictions.

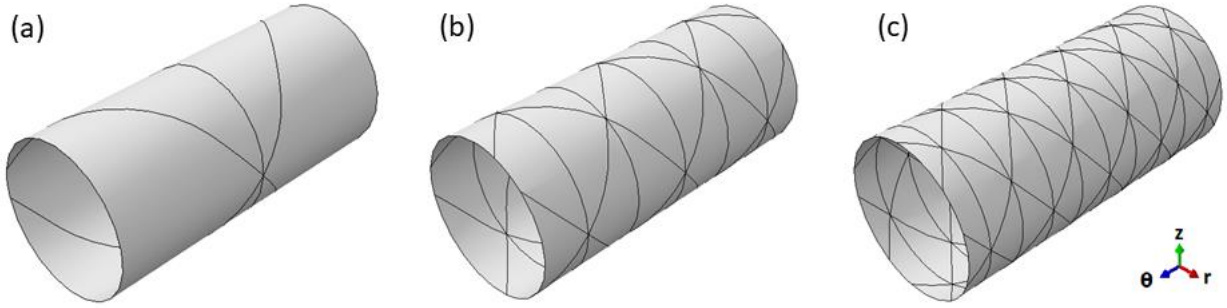

Figure 4 - $[\pm 50]_{FW}$ cylindrical shells with winding pattern (a) 1/1; (b) 3/1; and (c) 5/1.

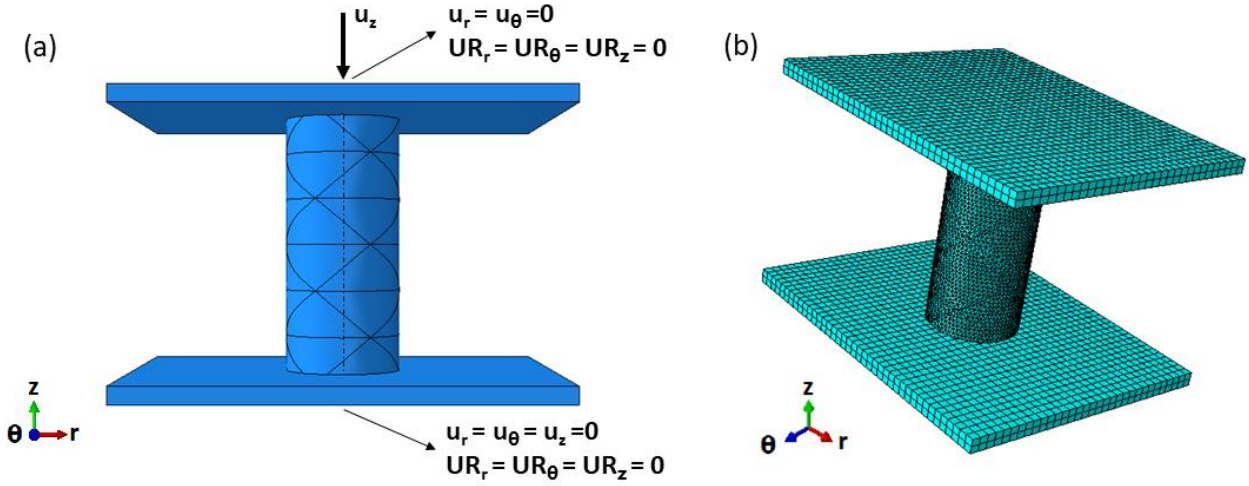

Figure 5: Assembly of the non-linear buckling model with boundary conditions (a); and typical mesh (b).

Damage analysis

The same FE model presented in the non-linear buckling section is herein utilized, however the Step of the analysis is replaced with a static one in order to predict the response of the cylinder considering progressive damage. Hashin failure criterion (Hashin, 1980) is used to capture damage initiation, where four failure modes can be identified: fiber tension, fiber compression, matrix tension, and matrix compression.

RESULTS AND DISCUSSION

Numerical results

The Figure 6 shows a mesh sensitivity analysis for an angle-ply $[\pm 50]_{FW}$ composite cylinder using a linear buckling model. The critical buckling loading converges reasonably well for a mesh with an element size of 2 mm. This element size was used in the modeling of the other patterns.

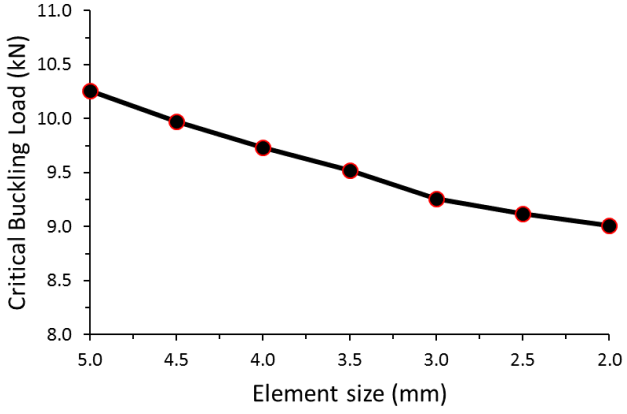

Figure 6: Mesh sensitivity for the $[\pm 50]_{FW}$.

Figure 7 shows load *vs.* displacement numerical and representative experimental curves. Experimental curves, test results, and photographs of the cylinders presented on this section were obtained in Azevedo et. al., 2019, which showed that the curves for different winding patterns are similar, which indicates that the winding pattern does not change the failure mode of the cylinders, but it is noted that the axial compressive behavior of the cylinders is sensitive to the mosaic winding pattern.

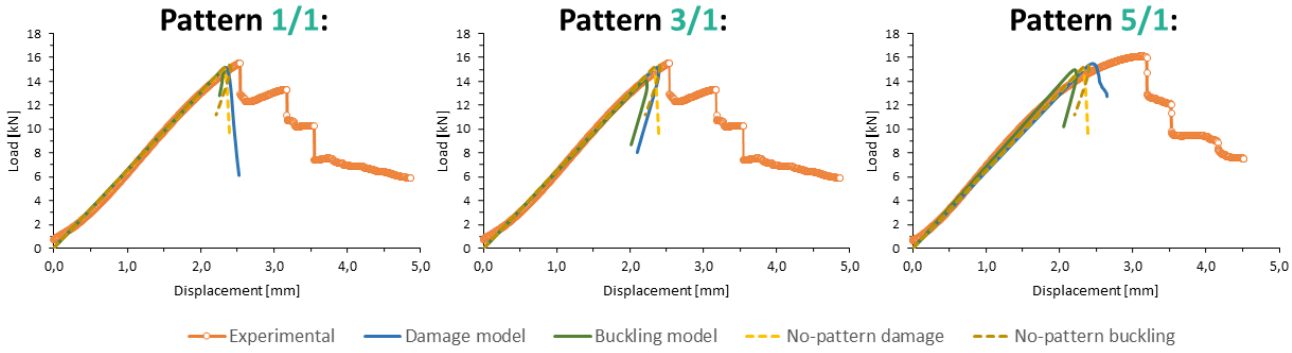

Figure 7: Load vs. displacement curves for the composite cylinders.

Analyzing Figure 8, it is possible to see that the numerical model is able to capture the compression damage accurately in relation to the experimental results. This is clear in the patter 1/1, where the initiation of the damage occurred in the central region of the cylinder, in the same region where the damage occurred in the test sample, where buckling started near the zig-zag area. In pattern 3/1 and 5/1 the damage occurs in a distributed way along the unit cells, which agrees with the numerical model, which presented distributed damage zones. In addition, a good correspondence with the experimental data was observed in the numerical model in the prediction of loading along the displacement history.

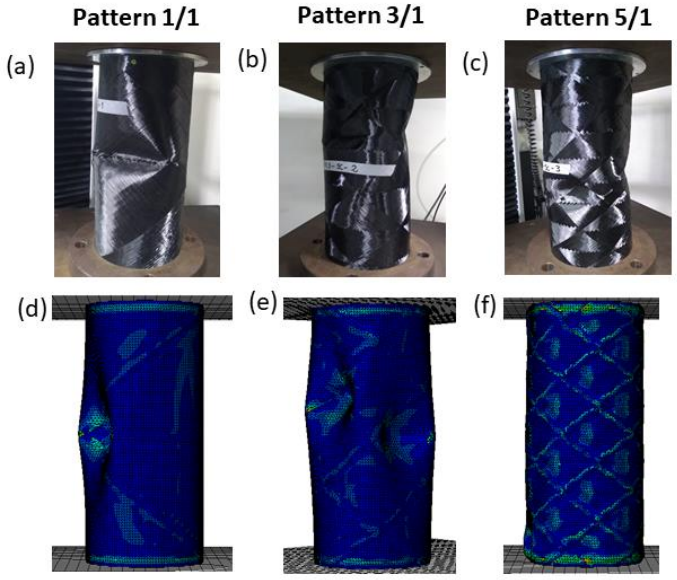

Figure 8 – Buckling shapes and final aspect of the damaged cylinders: experimental (a-c) vs. numerical (d-f) predicted with the damage model.

Table 2 shows the maximum loads and displacements obtained experimentally and numerically. The experimental results show the mean and standard deviation of three samples tested from each winding pattern. In the numerical model, the initial damage occurs suddenly, whereas the experimental curve may present a nonlinear region before the point of failure, due to the presence of imperfections in the structure, and fiber interlacing effects, which can cause the onset damage and the critical buckling load to not coincide. It is observed that in the 1/1 pattern, where there is no visible nonlinearity, there was a good correspondence between numerical and experimental results. In pattern 3/1 and 5/1, there were greater differences in the prediction of maximum load and maximum buckling displacement. However, the damage in the numerical model occurred at the beginning of the nonlinear region of the experimental curve, which shows that the model is able to predict damage initiation before buckling damage occurs in the structure.

Table 2: Experimental and numerical buckling loads and displacements.

Modeling	*Thickness (mm)*	*Load [kN]*			*Displacement [mm]*		
		Experim.	*Damage*	*Buckling*	*Experim.*	*Damage*	*Buckling*
Conventional	-	-	15.026	15.361	-	2.20	2.38
1/1	0.96	14.89 ± 2.09	15.181 (+1.02%)	15.123 (-1.57%)	2.41 ± 0.25	2.34 (+5.98%)	2.32 (-2.58%)
3/1	0.97	19.239 ± 1.13	15.141 (+0.75%)	14.041 (-9.4%)	3.10 ± 0.15	2.36 (+6.77%)	2.2 (-8.18%)
5/1	0.82	17.037 ± 1.60	15.440 (+2.68%)	14.990 (-2.47%)	3.26 ± 1.16	2.46 (+10.56%)	2.2 (-8.18%)

CONCLUSIONS

In this study, the winding pattern was modeled in order to determine the mechanical response of FW cylindrical shells subjected to axial compression loads. In order to predict the progressive damage, Hashin's model was used, whereas a non-linear buckling model based on the arc-length method was used to predict the buckling response of the cylinders.

A difference between the critical buckling load (experimental) and the onset of damage (numerical) load of 21.30% and 9.37%, respectively, was observed in patterns 3/1 and 5/1. It is possible to observe in the experimental curves that these patterns present a non-linearity before reaching the critical buckling load. This nonlinearity can occur due to robustness of the testing apparatus and the accommodation of the cylinder between the plates. Both models reproduced the experimental test very well in the elastic portion and the maximum compressive load. However, as none of the models taken delaminations into account, the numerical models were not able to predict the minor load drops after the maximum load was reached. For that, a 3D damage model should be employed.

ACKNOWLEDGMENTS

The authors would like to thank CAPES, CNPQ and FAPERGS. JHS Almeida Jr. is grateful to CAPES and Alexander von Humboldt for the financial support.

REFERENCES

Almeida Jr., J. H. S., Faria, H., Marques, A. T., Amico, S. C., 2014, "Load sharing ability of the liner in type III composite pressure vessels under internal pressure". Journal of Reinforced Plastics and Composites, Vol. 33, No. 24.

Almeida Jr., J. H. S., Ribeiro, M. L., Tita, V., Amico, S.C., 2016, "Damage and failure in carbon/epoxy filament wound composite cylinders under external pressure: experimental and numerical approaches". Materials & Design, Vol. 96, pp 431-438.

Almeida Jr., J. H. S., Tonatto, M. L. P., Ribeiro, M. L., Tita, V., Amico, S. C., 2018, "Buckling and post-buckling of filament wound composite cylinders under axial compression: linear, nonlinear, damage and experimental analyses". Composites Part B: Engineering, Vol. 159, pp. 227-239.

Azevedo, C. B., Eggers, F., Almeida Jr., J. H. S., Amico, S. C., 2018 "Effect of the filament winding pattern modeling on the axial compression of the cylindrical shells" Proceedings of the 4th Brazilian Conference on Composite Materials, Rio de Janeiro, pp 554-561

Azevedo, C. B, Flores, H. F., Almeida Jr., J. H. S., Eggers, F., Amico, S. C., 2019, "Influence of hygrothermal conditioning on axial compression of filament wound cylindrical shells". Proceedings of the 7th International Symposium on Solid Mechanics, V. Tita, A. Ferreira, M.L. Ribeiro, A. Vieira and A.T. Beck (Editors), ABCM, Sao Carlos, SP, Brazil, pp. 1-7.

Crisfield, M. A., 1981, "A fast incremental/iterative solution procedure that handles 'snap-through'". Computers & Structures, Vol. 13, Issues 1-3, pp. 55-62.

Hashin Z. Failure Criteria for Unidirectional Fiber Composites. J Appl Mech 1980;47(2):329-334.

Hernández-Moreno, H., Douchin, B., Collombet, F., Choqueuse, D., Davies, P., 2008, "Influence of winding pattern on the mechanical behavior of filament wound composite cylinders under external pressure". Composites Science and Technology, Vol. 68, Issues 3-4, pp. 1015-1024.

Morozov, E., 2006, "The effect of filament-winding mosaic patterns on the strength of thin-walled composite shells". Composite Structures, Vol. 76, No. 1-2, pp. 123-129.

Mian, H., Rahman, H., 2011, "Influence of mosaic patterns on the structural integrity of filament wound composite pressure vessels", International Journal of Structural Integrity, Vol. 2, No. 3, pp. 345-356.

Riks, E., 1979, "An incremental approach to the solution of snapping and buckling problems", International Journal of Solids and Structures, Vol. 15, No. 7, pp. 529-551.

Rousseau, J., Perreaus, D., Verdière, N., 1999, "The influence of winding patterns on the damage behaviour of filament-wound pipes", Composites Science and Technology, Vol. 59, No. 9, pp. 1439-1449.

Xia, M., Takayanagi, H., Kemmochi, K. 2001, "Analysis of multi-layered filament-wound composite pipes under internal pressure", Composite Structures, Vol. 53, No. 4, pp. 483-491.

Zu, L., He, Q., Shi, J., Li, H., 2013, "Non-geodesic trajectories for filament wound composite truncated conical domes". Applied Mechanics and Materials, Vol. 281, pp. 304-307.

RESPONSIBILITY NOTICE

The author(s) is (are) the only responsible for the printed material included in this paper.